

Monte Carlo Simulations for Assessment of Organ Radiation Doses and Cancer Risk in Patients Undergoing Abdominal Stent-graft Implantation

M.A. Blaszak ^{a,*}, R. Juszkat ^{b,c}

^a Adam Mickiewicz University, Faculty of Physics, Department of Biomedical Physics, Poznan, Poland

^b Department of General and Interventional Radiology, University of Medical Sciences, Poznan, Poland

^c Department of Neuroradiology, University of Medical Sciences, Poznan, Poland

WHAT THIS PAPER ADDS

In the literature, there are a limited number of studies reporting data concerning dose area product to patients undergoing abdominal stent-graft implantation. None of these papers report specific organ doses. In this paper, absorbed radiation doses in selected organs and cancer/mortality risks were estimated. In particular age, gender, and anatomical parameters of patients' aneurysms and arteries were considered. CALDose_X software was used, which improves on earlier software tools, which were mostly based on mathematical MIRD5-type phantoms.

Objectives and design: The aim of this work was to assess absorbed radiation doses in selected organs and to estimate cancer and mortality risks in patients undergoing abdominal stent-graft implantation, as a function of age, gender, and anatomical parameters of patients' aneurysms and arteries.

Materials and methods: 297 patients (266 males and 31 females) underwent endovascular aortic aneurysm repair (EVAR) with abdominal stent-graft implantation. Kerma—area products Gy·cm² for all implanted patients were collected retrospectively. Entrance surface air kerma (ESAK), doses absorbed by selected organs, and cancer/mortality risks were estimated using Monte Carlo simulation methods (CALDose_X software).

Results: The highest radiation doses were deposited in the skin, gallbladder wall, and colon wall. The highest average cancer risk was found for the youngest group of patients (<60 years old; 1:275) and the lowest for the oldest (>70 years old, 1:735). The radiation-induced risk of cancer mortality (mortality risk) was about 40% lower than radiation-induced cancer occurrence risk. Aneurysm neck angulations >45° had a significant impact on ESAK, as well as increasing cancer and mortality risks.

Conclusions: The main factors increasing cancer risk are young age and aneurysm neck angulations >45°, which determines the difficulty of proper stent-graft placement. However, the radiation risk associated with the stent-graft implantation procedure is relatively low, and EVAR should not be avoided.

© 2014 European Society for Vascular Surgery. Published by Elsevier Ltd. All rights reserved.

Article history: Received 26 June 2013, Accepted 20 March 2014, Available online 15 May 2014

Keywords: Radiation risk, Organ dose assessment, Stent-graft implantation, Aneurysm, Endovascular aortic aneurysm repair (EVAR)

INTRODUCTION

Endovascular aortic aneurysm repair (EVAR) was introduced as an alternative to open repair for the treatment of aortic aneurysms.^{1,2} It is less invasive than a surgical procedure and is widely used. In general, stent-grafting involves lower risks of complications and shorter hospital recuperation than traditional surgical operations in cases of pre-existing neurological, cardiovascular, pulmonary, or renal dysfunction. However, stent-graft implantation is a radiological

procedure that delivers relatively high radiation doses^{3–8} (Table 1).

The procedure may be coupled with extended exposure to X-rays for intervention planning, and manipulation of catheters and endovascular devices, as well as for long-term postoperative surveillance.⁹ Concern has been expressed regarding the radiation risks to both the patient and operator for fluoroscopically based interventional procedures.^{10,11}

The radiation dose, as the dose—area product or effective dose, associated with abdominal aortic stent-graft implantation is documented in only a few papers. None of them considers specific organ radiation doses for patients undergoing such a procedure.

X-ray examinations expose the human body to variable amounts of radiation. Depending on its location with respect to the boundaries of the irradiated body volume, a

* Corresponding author. M.A. Blaszak, Adam Mickiewicz University, Faculty of Physics, Department of Biomedical Physics, Ul. Umultowska 85, 61-614 Poznan, Poland.

E-mail addresses: blasaku@gmail.com; mklos@amu.edu.pl (M.A. Blaszak).

1078-5884/\$ — see front matter © 2014 European Society for Vascular Surgery. Published by Elsevier Ltd. All rights reserved.

<http://dx.doi.org/10.1016/j.ejvs.2014.03.014>

Table 1. Fluoroscopy time and DAP related to aneurysm repair.

	Number of patients	Mean fluoroscopy time (min)	Mean (median) DAP (Gy-cm ²)
Kalef-Ezra et al., 2009	62	23	42.5 (37.4)
Jones, et al., 2010	320	29	47 (no data)
Blaszak, et al., 2009	61	23	381 (355)
Geijer, et al., 2005	24	28	72 (60.1)
Panuccio, et al., 2011	47	83	782 (697)

specific organ or tissue can be exposed to primary radiation completely, partly, or not at all. Moreover, the long-term outcomes after endovascular repair are not as well documented as the long-term outcomes after open repair. In particular, the exact cancer and mortality risks associated with such treatments should be evaluated.

Practical dosimetric quantities such as ESAK (entrance surface air kerma; the kerma in air on the X-ray beam axis at the patient's skin) and KAP (air kerma—area product; the integral of air kerma across the entire X-ray beam emitted from the X-ray tube) are normally used to set absorbed doses and can be used as a means of risk assessment.^{12–15} The average dose to organs and tissues, as well as the cancer and mortality risks, can easily be assessed in virtual human phantoms using Monte Carlo (MC) methods.

MC simulation has become an accepted technique for solving radiation transport problems in many applications, including medical physics. CALDose_X (Department of Nuclear Energy, Federal University of Pernambuco, Recife, Brazil) is a software tool that assesses doses absorbed by organs and tissues of the human body and the associated cancer and mortality risks for radiographic examinations (an alternative to the effective dose, which cannot be used for an individual patient).^{16,17} The tissue-weighting factors applied in the calculation of the effective dose are calculated as gender- and age-averaged values and therefore effective dose cannot be used for the assessment of individual risk.¹⁸ Thus, the concept of effective dose for patients exposed to ionizing radiation from radiological procedures was not used in this study. Instead, the doses absorbed by selected organs and the cancer and mortality risks for patients undergoing abdominal stent-graft implantation as a function of gender, age, and anatomical parameters of aneurysms and arteries were calculated. CALDose_X improves on earlier software tools, which were mostly based on mathematical MIRD5-type phantoms, by using a less representative human anatomy.¹⁶

MATERIALS AND METHODS

Study design

In this study, measurements of KAP were simultaneously carried out from May 2006 to January 2013 on a sample of 297 adult patients (266 males and 31 females; 9% <60 years; 29% 61–70 years; 62% >70 years), who underwent abdominal stent-graft implantation. KAP, Gy-cm², for all implanted patients were collected retrospectively, and hence ethical approval was not required. Additionally,

aneurysm neck angulation (in degrees; the angle formed between the flow axes of the neck and body of the aneurysm) and the occurrence of iliac tortuosity were assessed (on the basis of CT performed before stent-graft implantation) in 93 patients (from May 2006 to January 2009) to determine whether either of these parameters affects radiation risks. All radiation data were analyzed retrospectively on the basis of archived information.

Risk calculations

CALDose_X (Department of Nuclear Energy, Federal University of Pernambuco, Recife, Brazil) is a Monte Carlo software tool that assesses doses absorbed by organs and tissues of the human body and the associated cancer and mortality risks for radiographic examinations (an alternative to the effective dose, which cannot be used for an individual patient).^{16,17} The tissue-weighting factors applied in the calculation of the effective dose are calculated as gender- and age-averaged values, and therefore effective dose cannot be used for the assessment of individual risk.¹⁸ Thus, the concept of effective dose for patients exposed to ionizing radiation from radiological procedures was not used in this study. Instead, the doses absorbed by selected organs and the cancer and mortality risks for patients undergoing abdominal stent-graft implantation as a function of gender, age, and anatomical parameters of aneurysms and arteries were calculated. CALDose_X improves on earlier software tools, which were mostly based on mathematical MIRD5-type phantoms, by using a less representative human anatomy.¹⁶

The absorbed dose can be defined by the ratio $E:m$, where E is the energy absorbed by the medium as a result of a beam of ionizing radiation being directed at a small mass, m . In X-ray examinations, the absorbed dose is the same as the equivalent dose (Gy). The absorbed dose in selected organs (mGy), ESAK, as well as cancer and mortality risks for average-sized male and female patients were calculated using CALDose_X. This program uses conversion coefficients (CCs) that were calculated using MASH (Male Adult meSH) and FASH (Female Adult meSH) human phantoms. Twenty-four different X-ray examinations with various projections can be simulated using spectra with 2.0–5.0 mm Al filtration between 60 and 150 kVp and different focus-to-detector distances (FDD). CALDose_X calculates CCs between organ and tissue absorbed doses, and also cancer incidence and mortality risks per kerma area product for the age defined by the user. An area of skin (7.2 × 7.2 cm), centred on the central axis of the X-ray beam, was used to calculate the entrance skin absorbed dose. The doses absorbed by the red bone marrow (RBM) and the bone surface cells (BSC) were calculated for those bones located inside the beam volume that showed the greatest values for such skeletal tissues. The cancer risks were calculated as “whole body effective risk”, which is the sum of risk-weighted organ absorbed doses using the risk factors given in the BEIR VII report.¹⁹ MC simulations were performed at appropriate peak potential (usually between 80 kVp and 90 kVp), actual beam filtration, focus-to-

detector distance (between 100 cm and 115 cm), and field position. Imaging was anterior–posterior (AP). The MC calculations were performed with 5 million source photons per examination.

Operative technique

All clinical procedures were performed with an operating C-arm unit (Allura, Philips Medical Systems, Best, The Netherlands) using pulsating X-ray radiation. COOK and GORE stent-graft were used. To prevent unexpected complications and to reduce unnecessary radiation exposure, accurate three-dimensional computed tomography was used before stent-graft implantation.

Stent-grafts (SGs) were implanted in conventional fashion from the right side with contra limb cannulation from the left to complete the procedure. Access was by open cut-down technique.

Statistical analysis

Results were analysed using the Mann–Whitney and Kruskal–Wallis tests, according to subgroups based on gender, age, aneurysm neck angulation (in degrees), and occurrence of iliac tortuosity. A p value $<.05$ was considered significant.

RESULTS

The mean KAP was 271 Gy-cm² in males (range 37–1760 Gy-cm²) and 276 Gy-cm² in females (range 64–625 Gy-cm²). The mean ESAK was 517 mGy for males (range 68–3219 mGy) and 374 mGy for females (range 39–1109 mGy). In 32% of patients ESAK was between 0.5 Gy and 1 Gy, and in 7% of patients, it exceeded 1 Gy (with a maximum observed value of 3.2 Gy). Absorbed doses for all radiated organs categorised by gender are shown in Table 2. The highest mean radiation doses were deposited in the skin (537 mGy in males, 380 mGy in females), gallbladder wall (299 mGy in males, 183 mGy in females), and colon wall (180 mGy in males, 142 mGy in females). There were significant differences between males and females for colon wall, lungs, pancreas, skin entrance, stomach, and gallbladder wall.

Cancer incidence and mortality risk per 100,000 cases are presented in Fig. 1. Despite lower risk coefficients for the gender-specific organs in males, the difference in cancer risk between male and female patients was statistically insignificant ($U = 3416$, $p = .13$; Mann–Whitney test). The highest mean cancer risk was found for the youngest group of patients (<60 years old) and was 364 per 100,000 cases (1:275) and the lowest, 136 per 100,000 cases, for patients >70 years old (1:735) (Fig. 1). The differences between all age groups were highly significant ($H = 62.6$, $df = 2$, $p < .00001$; Kruskal–Wallis test). The highest observed cancer risk (1:66) was found for a 58-year-old male patient in whom the deposited entrance surface air kerma was 2599 mGy-cm². In general, mortality risks for both genders were about 40% lower than cancer risks and with aging, risk coefficients decreased significantly ($H = 36.4$, $df = 2$,

Table 2. Radiation doses absorbed by organs and tissues in patients anatomically similar to the Male Adult meSH (MASH) and the Female Adult meSH (FASH) phantoms categorised by gender.

	Absorbed dose (SE) [mGy]		p (Mann–Whitney test)
	Male	Female	
ESAK	517 (24)	374 (40)	.02
Adrenals	23.4 (1)	28.2 (3.2)	.11
Bladder wall	79 (3.6)	89 (9.9)	.25
Colon wall	180 (8.2)	142 (15.8)	.08
Breasts, glandular	—	5.9 (0.7)	—
Kidneys	38.4 (1.7)	31.9 (3.7)	.20
Liver	114 (5.2)	89.4 (10.2)	.11
Lungs	3.7 (0.2)	4.6 (0.5)	.04
Oesophagus	4.2 (0.2)	5 (0.6)	.14
Testes/ovaries	7.7 (0.4)	80 (9.2)	—
Pancreas	162 (7.4)	97 (11.1)	.0003
Small intestine wall	174 (8)	134 (15.4)	.08
Skin entrance 7.2 cm × 7.2 cm	537 (25)	380 (43)	.02
Spleen	68.4 (3.1)	64.3 (7.4)	.80
Stomach wall	177 (8.1)	118 (13.5)	.004
Prostate	27.4 (1.2)	—	—
Uterus	—	60.5 (7)	—
Heart wall	4.7 (0.2)	6 (0.7)	.05
Lymphatic nodes	72 (3.3)	68.5 (7.9)	.90
Gallbladder wall	299 (13.7)	183 (21)	.0006
Skeleton average	41.6 (1.9)	43.8 (5.1)	.52
Maximum RBM absorbed dose	41 (1.9)	39.9 (4.6)	.98
Maximum BSC absorbed dose	53 (2.4)	52 (6.1)	.98
Weighted MASH/FASH dose	63 (2.9)	55 (6.3)	.41

RBM = red bone marrow; BSC = bone surface cells.

$p < .00001$; Kruskal–Wallis test). The calculations showed that aneurysm neck angulations $>45^\circ$ have a significant impact on cancer and mortality risk ($H = 6.5$, $df = 2$, $p = .04$, $H = 6.8$, $df = 2$, $p = .04$, respectively; Kruskal–Wallis test) (Fig. 1). The occurrence of iliac tortuosity had no influence on cancer and mortality risks ($U = 417$, $p = .16$; $U = 395$, $p = .10$, respectively; Mann–Whitney test).

DISCUSSION

Large surveys of radiation doses in patients undergoing X-ray examinations in diagnostic and interventional radiology are one method adopted by countries or regions with the aim of reviewing and recommending diagnostic reference levels. For this reason, the study of radiation doses that patients receive during various (especially long-lasting) procedures is highly important. The available data suggest that radiation exposure during endovascular aneurysm repair might be high.^{20,21} All patients should be monitored for 3 months post-procedurally to look for the appearance of radiation sickness (e.g. multiple blood tests, and clinical interview).

Diseases such as arterial stenosis or high blood pressure necessitate higher doses of ionic radiation, causing problems with the positioning and deployment of the prosthesis.²¹

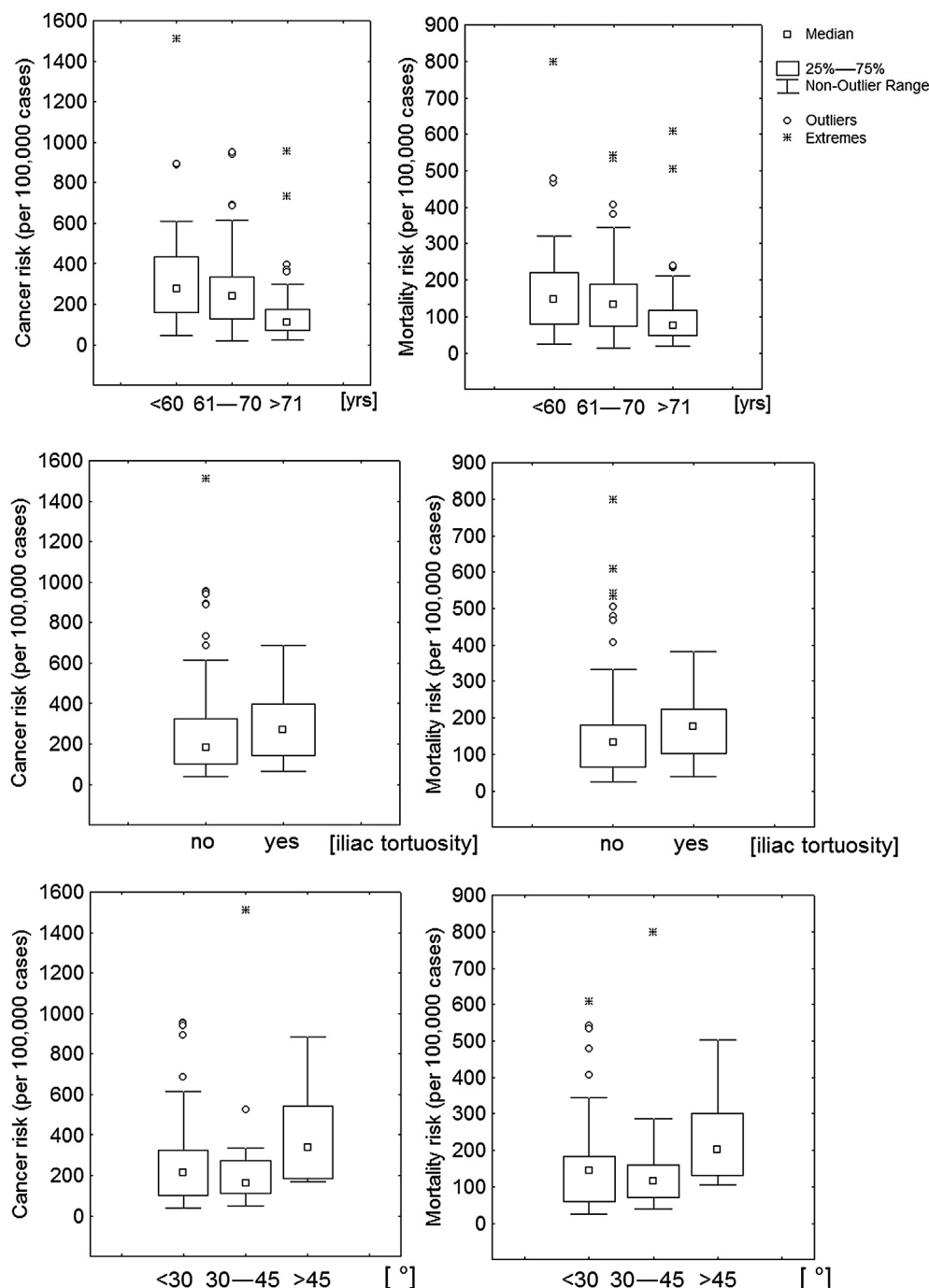


Figure 1. The radiation-induced risk of cancer mortality (mortality risk) and cancer incidence as a function of gender, age, occurrence of iliac tortuosity, and aneurysm neck angulations.

The time required for stent-graft implantation is influenced by the anatomy of the aorta and iliac arteries. For example, it is sometimes difficult and time-consuming to deliver the stent-graft safely through a tortuous iliac artery. The correct location of the stent-graft requires precision and may prolong the length of the operation – influencing the radiation dose. This study has shown that angulations exceeding 45° require more precise implantation of the main body of the graft. Moreover, this requires more angulations of the image intensifier and contributes to a greater overall dose of radiation.

In the literature, there are a limited number of studies reporting data concerning KAP (or DAP) in such procedures. For those which are available, the spread of the DAP values is very large and none report specific organ doses. Kalef-Ezra et al.⁹ have reported mean DAP values ranging from 30 to 782 Gy cm² (which is two times higher than the value presented here). A trigger level of 300 Gy cm² was proposed by Neofotistou.²² This value, in the case of complex procedures such as stent-graft implantation, is exceeded in more than 35% of cases (in our study).

In general, risks associated with ionizing radiation can be divided into stochastic and deterministic effects. Stochastic effects are chance events, with the probability of the effect increasing with dose, but the severity of the effect is independent of the dose received (genetic risks in offspring or somatic effects like cancer). Deterministic effects are related directly to the absorbed radiation dose and the intensity of the effect increases as the dose increases. Deterministic effects have a threshold below which the effect does not occur and are based on tissue damage.

The probability of induction of stochastic effects is related to the weighted sum of the doses absorbed in various organs and tissues specified by ICRP.¹⁸ Our simulations showed that the mean cancer risk associated with stent-graft implantation is relatively low (average: 136–364 per 100,000 cases). It is related to the fact that most EVAR patients are above the age of 65 (age-related risk coefficients decrease with aging), and deterministic injuries are usually of greater concern than those of stochastic effects. It has been shown that the highest mean cancer risk was found for the youngest group of patients and with aging, risk coefficients decreased significantly. The highest observed cancer risk (1:66) was found for a 58-year-old male patient in whom the deposited entrance surface air kerma was 2599 mGy·cm². Therefore, radiation-induced cancer risks in the young also constitute a potential contra-indication to EVAR in this group.

The fact that complications of endovascular therapy can occur early or be delayed means that life-long imaging follow-up is required. Typical follow-up imaging management consists of a CT examination performed within the first month after stent-graft placement. As complications such as endoleak, aneurysm sac expansion, and graft migration may occur long after the stent-graft is placed, imaging surveillance must be lifelong.^{23,24} In this work the cancer and mortality risks associated only with the completed operation were calculated. The total cancer risk will be slightly greater overall, and will depend on the total radiation dose that the patient receives, including the periodic assessments after stent-graft implantation. Moreover, it should be noted that the cancer risk for patients depends on various factors, such as a number of equipment-related variables including beam collimation, servicing, filter usage, movement capabilities of the X-ray source, fluoroscopic specifications (pulse rate, acquisition frame rate, and acquisition input dose rates), the position of the projection and potential variations in the skill of the operator.²⁵

EVAR might be accomplished in an operating theatre using a mobile C-arm for X-ray guidance or in a dedicated angiographic suite using fixed equipment. It was thought that the mobile C-arm might lead to higher patient doses because of greater operational difficulties and higher staff doses as it produces a less focused beam with a wider scatter of X-rays, compared with dedicated angiographic equipment.⁴ On the other hand, Fossaceca et al.²⁶ demonstrated that EVAR performed using a fluoroscopy C-arm resulted in a very low patient radiation dose. The patient's radiation dose increases by at least one order of

magnitude when using mobile or fixed angiographic equipment, whereas the clinical outcomes are equivalent. Further studies from other research centres (ideally using different machinery and other operators) are required to verify these findings.

Conclusions

This study determined radiation doses in selected organs and estimated cancer and mortality risks using Monte Carlo methods in patients undergoing abdominal stent-graft implantation as a function of age, gender, and anatomical parameters of patients' aneurysms and arteries.

Consequently, the X-ray doses absorbed by specific organs and the associated cancer risk are not very high, but are significant. It has been shown that average cancer risk ranges from 364 per 100,000 cases (1:275) in the youngest patients (<60 years) to 136 per 100,000 cases (1:735) in the oldest (>70 years). The main factors increasing cancer risk are young age and aneurysm neck angulations >45°, which determines the difficulty of proper stent-graft placement. However, the radiation risk associated with the stent-graft implantation procedure is relatively low, thus even in these cases EVAR should not be avoided.

FUNDING

None.

CONFLICT OF INTEREST

None.

REFERENCES

- 1 Schermerhorn ML, O'Malley AJ, Jhaveri A, Cotterill P, Pomposelli F, Landon BE. Endovascular vs. open repair of abdominal aortic aneurysms in the Medicare population. *N Engl J Med* 2008;**358**(5):464–74.
- 2 Kapma MR, Verhoeven ELG, Tielliu IFJ, Zeebregt CJAM, Prins TR, Van der Heij B, et al. Endovascular treatment of acute abdominal aortic aneurysm with a bifurcated stent-graft. *Eur J Vasc Endovasc Surg* 2005;**29**(5):510–5.
- 3 Kalef-Ezra JA, Karavasilis S, Ziogas D, Dristiliaris D, Michalis LK, Matsagas M. Radiation burden of patients undergoing endovascular abdominal aortic aneurysm repair. *J Vasc Surg* 2009;**49**(2):283–7.
- 4 Jones C, Badger SA, Boyd CS, Soong CV. The impact of radiation dose exposure during endovascular aneurysm repair on patient safety. *J Vasc Surg* 2010;**52**(2):298–302.
- 5 Panuccio G, Greenberg RK, Wunderle K, Mastracci TM, Engelson MG, Davros W. Comparison of indirect radiation dose estimates with directly measured radiation dose for patients and operators during complex endovascular procedures. *J Vasc Surg* 2011;**53**:885–94.
- 6 Blaszk MA, Majewska N, Juszkat R, Majewski W. Dose-area product to patients during stent-graft treatment of thoracic and abdominal aortic aneurysms. *Health Phys* 2009;**97**(3):206–11.
- 7 Howells P, Eaton R, Pate AS, Taylor P, Modarai B. Risk of radiation exposure during endovascular aortic repair. *Eur J Vasc Endovasc Surg* 2012;**43**(4):393–7.

- 8 Geijer H, Larzon T, Popek, Beckman RKW. Radiation exposure in stent-grafting of abdominal aortic aneurysms. *Br J Radiol* 2005;**78**:906–12.
- 9 Kalef-Ezra JA. *Endovascular repair: radiation risks, aneurysmal disease of the thoracic and abdominal aorta*. InTech; 2011, ISBN 978-953-307-578-5.
- 10 Miller DL, Balter S, Cole PE, Lu HT, Schueler BA, Geisinger M, et al. Radiation doses in interventional radiology procedures: the RAD-IR study: part I: overall measures of dose. *J Vasc Interv Radiol* 2003;**14**:711–27.
- 11 Hausler U, Czarwinski R, Brix G. Radiation exposure of medical staff from interventional x-ray procedures: a multicentre study. *Eur Radiol* 2009;**19**:2000–8.
- 12 Hart D, Jones DG, Wall BF. *Normalized organ doses for medical X-ray examinations calculated using Monte Carlo techniques*. NRPB-SR262; 1994.
- 13 Hart D, Jones DG, Wall BF. *Coefficients for estimating effective doses for pediatric X-ray examinations*. NRPB-R279; 1996.
- 14 IAEA. *Technical reports series 457. Dosimetry in diagnostic radiology: an international code of practice*. International Atomic Energy Agency; 2007.
- 15 ICRU. *Report 74. Patient dosimetry for X-rays used in medical imaging*. International Commission on Radiation Units and Measurements; 2005.
- 16 Kramer R, Khoury HJ, Vieira JW. CALDose_X — a software tool for the assessment of organ and tissue absorbed doses, effective dose and cancer risks in diagnostic radiology. *Phys Med Biol* 2008;**53**:6437–59.
- 17 Kramer R, Cassola VF, Khoury HJ, Vieira JW, Lima VJ, Brown KR. FASH and MASH: female and male adult human phantoms based on polygon mesh surfaces: II. Dosimetric calculations. *Phys Med Biol* 2010;**55**:163–89.
- 18 The 2007 recommendations of the International Commission on Radiological Protection. *Ann ICRP* 2007;**37** [publication no. 103].
- 19 National Research Council. *Health risks from exposure to low levels of ionizing radiation — BEIR VII*. Washington DC: The National Academies Press; 2005.
- 20 Greenhalgh RM, Brown LC, Kwong GP, Powell JT, Thompson SG. Comparison of endovascular aneurysm repair with open repair in patients with abdominal aortic aneurysm (EVAR trial 1), 30-day operative mortality results: randomized controlled trial. *Lancet* 2004;**364**:843–8.
- 21 Majewska N, Juszkak R, Blaszkak M, Frankiewicz M, Makalowski M, Stanisic M, et al. Abdominal aorta aneurysm: case report of high radiation dose during stent-graft implantation. *Pol J Radiol* 2011;**76**(4):60–2.
- 22 Neofotistou V, Vaňo E, Padovani R, Kotre J, Dowling A, Toivonen M, et al. Preliminary reference levels in interventional cardiology. *Eur Radiol* 2003;**13**:2259–63.
- 23 Macari M, Chandarana H, Schmidt B, Lee J, Lamparello P, Babb J. Abdominal aortic aneurysm: can the arterial phase at CT evaluation after endovascular repair be eliminated to reduce radiation dose? *Radiology* 2006;**241**(3):908–14.
- 24 Tolia AJ, Landis R, Lamparello P, Rosen R, Macari M. Type II endoleaks occurring after endovascular repair of abdominal aortic aneurysms: natural history. *Radiology* 2005;**235**:683–6.
- 25 Walsh SR, Cousins C, Tang TY, Gaunt ME, Boyle JR. Ionizing radiation in endovascular interventions. *J Endovasc Ther* 2008;**15**:680–7.
- 26 Fossaceca R, Brambilla M, Guzzardi G, Cerini P, Renghi A, Valzano S, et al. The impact of radiological equipment on patient radiation exposure during endovascular aortic aneurysm repair. *Eur Radiol* 2012;**22**(11):2424–31.